

**SIMULTANEOUS EXTRACTION OF MULTIPLE PARAMETERS FROM A TRANSMIT-RECEIVE EDDY CURRENT PROBE ABOVE A LAYERED PLANAR CONDUCTIVE STRUCTURE**

**M. S. Luloff<sup>1</sup> S. Contant, T. W. Krause**  
Royal Military College of Canada  
Kingston, Canada

**J. Morelli**  
Queen's University  
Kingston, Canada

**ABSTRACT**

*A validated analytical model of a transmit-receive eddy current (EC) coil pair, situated above two parallel plates, separated by an air gap, was used as the basis for an Inversion Algorithm (IA) to extract probe liftoff, second layer plate resistivity, and plate-to-plate gap from multi-frequency EC data. The IA was tested over a large range of first layer wall thickness (3.80 mm and 4.64 mm), second layer plate resistivity (1.7-174  $\mu\Omega\cdot\text{cm}$ ), second layer wall thickness (1.20 mm to 4.85 mm), probe liftoff (2.8 mm to 7.9 mm), and plate-to-plate gap (0 mm to 13.3 mm). At nominal liftoff (2.8 mm) the IA achieved a gap measurement accuracy of  $\pm 0.7$  mm, and was able to return good estimates of second layer resistivity to within  $\pm 1$   $\mu\Omega\cdot\text{cm}$  for low resistivity samples, but decreasing accuracy for higher resistivity. When gap was fixed, the IA was able to measure changes in probe liftoff (relative to nominal) to an accuracy of  $\pm 0.2$  mm. The reported accuracy and a demonstration of the ability to accurately estimate parameters outside of the calibration range provides confidence in the potential utility of the algorithm.*

Keywords: Eddy current testing, Inversion problem, multi-frequency, non-destructive testing

**NOMENCLATURE**

EC	Eddy Current
FP	Far Plate
IA	Inverse Algorithm
NP	Near Plate
TR	Transmit-Receive
WT	Wall Thickness

**1. INTRODUCTION**

A number of industrial applications require knowledge of the separation or gap between two conducting surfaces. For example, in heavy water nuclear reactor fuel channels, the gap between pressure tubes (PTs) and surrounding calandria tubes

(CTs) requires regular monitoring to avoid contact conditions, which may result in delayed hydride cracking of the PT [1]. Eddy Current (EC) testing using a transmit-receive (TR) probe (two horizontally offset coils) with axes oriented perpendicular to the inner face of the PT has proven to be effective for in-reactor inspection. However, variation in probe liftoff and PT resistivity have the potential to affect the accuracy of the EC-based gap measurement [2]. A representation of the probe geometry and associated boundary value problem is shown in Figure 1. The flat-plate approximation of the fuel channel tubes is suitable, since the radii of real PTs and CTs are much larger than the probe dimensions, and therefore, yield an excellent approximation of the signal response. Shokralla et al. [3] confirmed the validity of this approximation for excitation frequencies greater than 4 kHz. The flat-plate equivalents of the PT and CT are denoted here as the Near Plate (NP) and Far Plate (FP), respectively. In previous work [4], an analytical model of the EC probe above two parallel plates, separated by an air gap was developed to simulate the probe's response. The model was found to be in excellent agreement with experiment.

Model-based inversion and in-particular, the volume-integral method, is a commonly applied technique used to estimate measurement parameters [5]. In this work, an algorithm that simultaneously extracts unknown parameters from EC measurements was developed for a TR probe configuration above two layered conducting plates by finding the least-squares error between the analytical model and measurements. This inverse algorithm (IA) was found to return an accurate gap measurement despite variances in probe liftoff and plate resistivity.

**2. MATERIALS AND METHODS**

The same experimental samples used in Ref. [4] were used in this work, which are summarized below in Table 1. For the purposes of this work, a 3.80 mm (Sample A) or 4.64 mm (Sample G) thick Grade 5 6AL-4V titanium sheet was used as the NP. Copper, brass, aluminum, non-ferromagnetic SS-316 stainless-steel, Grade 2 titanium, and Grade 5 6AL-4V Titanium

<sup>1</sup> Contact author: mark.luloff@cnl.ca

samples were used as the FPs, which provided a large range of material resistivity and wall thickness to test the IA. As stated in Ref. [4], the wall thicknesses of the samples were determined by ultrasonic methods, and their resistivities were determined by a combination of EC based methods [4] and four-point measurements. Table 1 shows the sample characteristics, which were used in a previous study [4].

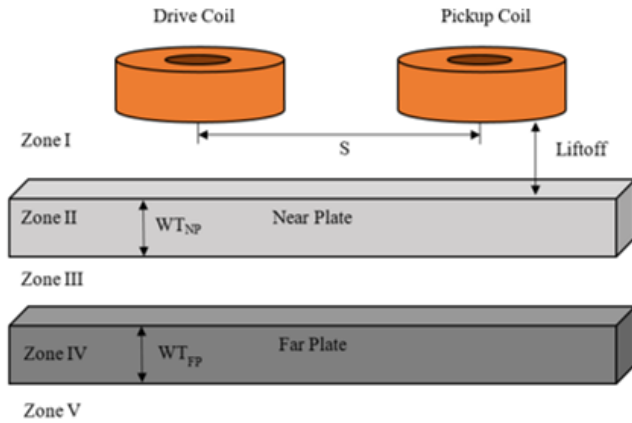


**FIGURE 1:** TRANSMIT-RECEIVE PROBE ABOVE LAYERED PLANAR TEST-PIECE

**TABLE 1:** RESISTIVITY AND WALL THICKNESS OF PLATE SAMPLES

Sample	Material	Measured Resistivity [ $\mu\Omega\cdot\text{cm}$ ] at $20.0\pm 0.5\text{ }^\circ\text{C}$	Thickness [mm] to $2\sigma$
A	Grade 5 Ti-6Al-4V	174	$3.80\pm 0.08$
B	Grade 5 Ti-6Al-4V	$174\pm 2$	$4.26\pm 0.08$
C	Brass (Copper-Zinc alloy)	6.2	$3.30\pm 0.04$
D	Copper	1.7	$1.65\pm 0.04$
E	Aluminum	4.5	$4.85\pm 0.02$
F	SS-316 Stainless Steel	$74.5\pm 0.7$	$1.20\pm 0.01$
G	Grade 5 Ti-6Al-4V	174	$4.64\pm 0.01$
H	Grade 2 (pure) Titanium	53.9	$3.18\pm 0.01$

The EC probe was fixed to either Sample A (Grade 5 6Al-4V Titanium) as the NP at nominal liftoff ( $2.81\pm 0.05\text{ mm}$ ) in the absence of any FPs. The EC instrument was then nulled. This null reference point was chosen for experimental convenience. The probe and NP (either Sample A or G) were separated from any one of the FP samples by (up to thirteen)  $1.02\pm 0.05\text{ mm}$  thick plastic shims to create a precise air gap. Shims were removed, during time-based acquisition, to measure the plate-gap profile for the probe. Similarly, the liftoff profile was measured at a fixed NP-FP gap by progressively adding up to five shims to increase the probe liftoff, again during time-based acquisition, over a range of  $2.81\pm 0.05\text{ mm}$  to  $7.9\pm 0.3\text{ mm}$ .

### 3. RESULTS AND DISCUSSION

Experimental measurements were taken to validate the IA over a large range of experimental parameters. Figure 2 and Table 2 characterizes the IA-determined liftoff estimates at varying plate

gaps ( $1.02\pm 0.05$ ,  $2.0\pm 0.1$ ,  $3.1\pm 0.2$ , and  $4.0\pm 0.2\text{ mm}$ ), FP resistivity, and NP/FP WT.

**TABLE 2:** PREDICTED PLATE GAP OBTAINED FROM THE INVERSION ALGORITHM (IA) VERSUS ACTUAL PLATE GAP RESULTING FROM VARIATION IN FAR PLATE RESISTIVITY AND WALL THICKNESS AT NOMINAL LIFTOFF ( $2.81\text{ mm}$ )

NP	FP	$\rho_{FP}$ (Actual) [ $\mu\Omega\cdot\text{cm}$ ]	$\rho_{FP}$ (IA) $\pm 2\sigma$ [ $\mu\Omega\cdot\text{cm}$ ]	Gap (Actual) [ $\mu\Omega\cdot\text{cm}$ ]	Gap (IA) $\pm 2\sigma$ [mm]
A	F	$74.5\pm 0.7$	$73\pm 4$	$2.0\pm 0.1$	$2.3\pm 0.2$
A	D	1.7	$1.4\pm 0.3$	$4.1\pm 0.2$	$4.40\pm 0.02$
A	H	53.9	$49.6\pm 0.4$	$1.02\pm 0.05$	$1.22\pm 0.03$
G	F	$74.5\pm 0.7$	$73\pm 3$	$2.0\pm 0.1$	$2.4\pm 0.2$
G	D	1.7	$1.4\pm 0.3$	$3.1\pm 0.2$	$3.67\pm 0.02$
G	H	53.9	$49\pm 1$	$2.0\pm 0.1$	$2.50\pm 0.03$

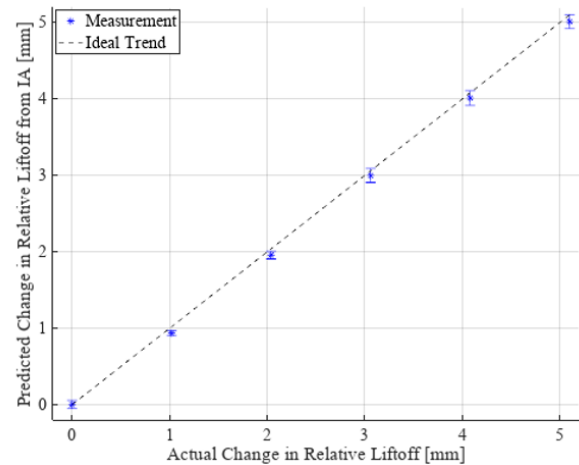


**FIGURE 2:** PREDICTED CHANGE IN PROBE LIFTOFF (FROM NOMINAL) OBTAINED FROM THE IA VERSUS THE ACTUAL CHANGE IN PROBE LIFTOFF

Lastly, Figure 3 characterizes the performance of the IA-determined gap measurement at nominal liftoff under varying NP/FP all thickness and FP resistivity. Similarly thirteen gap measurements (i.e.  $0\text{ mm}$ ,  $1.02\pm 0.05\text{ mm}$ ,  $2.0\pm 0.1\text{ mm}$ , ...,  $13.3\pm 0.8\text{ mm}$ ) for each combination of NP/FP WT and FP resistivity presented in Table 3 performed at nominal liftoff

As shown in Table 3, excellent agreement is observed between the experimental data and IA results. As shown in Table 2 and Table 3, the IA consistently predicts the LO within experimental uncertainty when both Samples A ( $3.8\text{ mm}$  thick Grade 5 Ti-6Al-4V) and G ( $4.6\text{ mm}$  thick Grade 5 Ti-6Al-4V) were used as NPs. From a linear regression of the data in Figure 3, it was found that the IA achieved a systematic uncertainty (the y-intercept of Figure 3) of  $+0.1\pm 0.1\text{ mm}$  (bounded by  $\pm 0.2\text{ mm}$ ), while the random uncertainty (determined from the error bars in Figure 3), was bounded within  $\pm 0.5\text{ mm}$  (two standard deviations) for the gap measurement at nominal liftoff ( $2.81\text{ mm}$ ). To ensure a conservative assessment, the bounding limits of the systematic error and random error were added. Therefore,

the absolute accuracy of the gap measurement was reported as  $\pm 0.7$  mm for the probe operated at nominal liftoff.

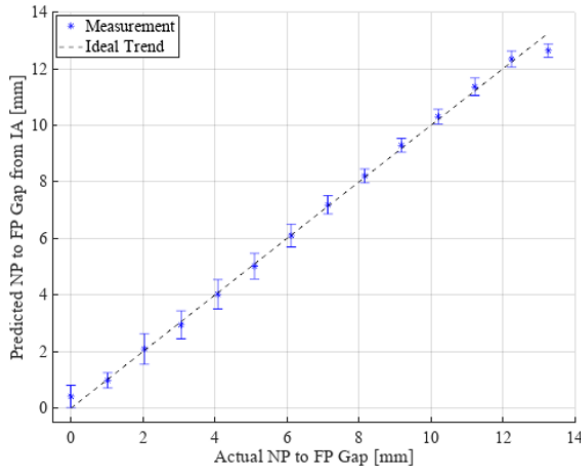


**FIGURE 3:** THE PREDICTED GAP OBTAINED FROM THE IA VERSUS THE ACTUAL GAP RESULTING FROM VARIATION IN FAR PLATE RESISTIVITY AND WALL THICKNESS AT NOMINAL LIFTOFF (2.81 mm)

**TABLE 3:** INVERSION ALGORITHM (IA) RESULTS FOR MEASURED GAP PROFILES FROM 0 MM TO  $13.3 \pm 0.7$  mm AT A NOMINAL LIFTOFF OF  $2.81 \pm 0.05$  mm

NP	FP	$\rho_{FP}$ (Actual) [ $\mu\Omega\cdot\text{cm}$ ]	$\rho_{FP}$ (IA) $\pm 2\sigma$ [ $\mu\Omega\cdot\text{cm}$ ]	LO (IA) $\pm 2\sigma$ [mm]
A	D	1.7	$1.6 \pm 0.3$	$2.81 \pm 0.03$
A	H	53.9	$50.4 \pm 0.6$	$2.81 \pm 0.02$
A	E	4.5	$4.99 \pm 0.0$	$2.83 \pm 0.01$
A	F	$74.5 \pm 0.7$	$71 \pm 1$	$2.82 \pm 0.01$
A	C	6.2	$6.20 \pm 0.2$	$2.82 \pm 0.01$
A	B	$174 \pm 2$	$169 \pm 1$	$2.82 \pm 0.05$
A	G	$174 \pm 2$	$173 \pm 1$	$2.83 \pm 0.02$
A	D	1.7	$1.6 \pm 0.2$	$2.79 \pm 0.02$
A	F	$74.5 \pm 0.7$	$70.9 \pm 0.6$	$2.78 \pm 0.02$
G	D	1.7	$1.5 \pm 0.3$	$2.84 \pm 0.03$
G	E	4.5	$4.5 \pm 0.6$	$2.84 \pm 0.02$
G	F	$74.5 \pm 0.7$	$70 \pm 3$	$2.84 \pm 0.04$
G	H	53.9	$49.4 \pm 0.8$	$2.81 \pm 0.04$

When the liftoff was varied from 2.81 mm to 7.9 mm, the largest difference in the IA prediction of gap and experiment was largest when Sample G was the NP and Sample D was the FP, achieving an estimated  $3.67 \pm 0.01$  mm gap as opposed to the actual gap of  $3.1 \pm 0.2$  mm. From a linear regression of the data in Figure 2, it was found that the IA achieved a systematic error (the y-intercept of Figure 2) of  $-0.04 \pm 0.02$  mm (bounded by  $\pm 0.06$  mm) for the measured deviance in LO from nominal with the random uncertainty bounded within  $\pm 0.1$  mm (two standard deviations). Similarly, the uncertainty in the relative liftoff measurement was calculated by adding the bounding limits of the systematic and random error together. Therefore, the

uncertainty of the relative LO measurement achieved by the IA (after rounding) was reported as  $\pm 0.2$  mm.

#### 4. CONCLUSION

A robust Inversion Algorithm (IA) was developed to simultaneously extract probe liftoff, far-plate (FP) resistivity and gap from multi-frequency EC measurements. The IA was tested over a large range of first layer wall thickness (3.80 mm and 4.64 mm), second layer plate resistivity (1.7-174  $\mu\Omega\cdot\text{cm}$ ), second layer wall thickness (1.20 mm to 4.85 mm), probe liftoff (2.8 mm to 7.9 mm), and plate-to-plate gap (0 mm to 13.3 mm). In addition, at nominal liftoff the IA returned reasonable estimates of the FP resistivity; for the low resistivity samples (copper, aluminum and brass) the error in the FP resistivity is bounded by  $\pm 0.9$   $\mu\Omega\cdot\text{cm}$  and for the higher resistivity samples (grade 5 titanium, grade 2 titanium and stainless-steel), the FP resistivity is bounded by  $\pm 6$   $\mu\Omega\cdot\text{cm}$ . When the gap was fixed, the IA was able to measure changes in probe liftoff (relative to nominal) to an accuracy of  $\pm 0.2$  mm. The reported accuracy and a demonstration for the ability to accurately estimate parameters outside of the calibration range provides confidence in the potential utility of the algorithm.

#### ACKNOWLEDGEMENTS

The first author would like to thank Perryn Bennett for his assistance in reviewing this paper. Work was supported by the University Network of Excellence in Nuclear Engineering, Ontario Power Generation, and the Natural Sciences and Engineering Research Council of Canada.

#### REFERENCES

- [1] E.G. Price, "Highlights of the Metallurgical Behaviour of CANDU Pressure Tubes," AECL, Chalk River, Ontario, Nov. 1980.
- [2] S. Shokralla and T.W. Krause, 'Methods for Evaluation of Accuracy with Multiple Essential Parameters for EC Measurement of PT-CT Gap in CANDU® Reactors', CINDE Journal, 35, No. 1, Jan/Feb 2014, pgs. 5-8.
- [3] S. Shokralla, S. Sullivan, J. Morelli, and T.W. Krause, "Modelling and Validation of Eddy Current Response to Changes in Factors Affecting Pressure to Calandria Tube Gap Measurement," NDT & E International Vol. 73, 2015.
- [4] M.S. Luloff, J. Morelli and T. W. Krause, "Solution for a Transmit-Receive Eddy Current Probe above a Layered Planar Conductive Structure" NDT&E International, Vol. 96. pp.1-8, June 2018.
- [5] H. Sabbagh, R. Murphy, E. Sabbagh, J. Aldrin, J. Knopp and M. Blodgett, "Computational Electromagnetics and Model-Based Inversion: A Modern Paradigm for Eddy-Current Nondestructive Evaluation," *ACES Journal*, vol. 24, no. 6, pp. 533-540, 2009
- [6] V. S. Cecco, G. V. Drunen, and F. L. Sharp, "Eddy Current Testing Manual on Eddy Current Method," Atomic Energy of Canada Limited, Chalk River, Ontario, Canada, 1981.

